

Crystalline characterization by Rutherford backscattering spectrometry and electron channelling of *in situ* grown $\text{YBa}_2\text{Cu}_3\text{O}_7$ thin films deposited on (1 0 0) MgO by d.c. sputtering or laser ablation

M. KECHOUANE*, H. L'HARIDON, M. SALVI, P. N. FAVENNEC, M. GAUNEAU
CNET Lannion B, Route de Trégastel, BP 40, 22301 Lannion CEDEX, France

M. GUILLOUX-VIRY, M. G. KARKUT†, C. THIVET, A. PERRIN‡
Laboratoire de Chimie du Solide et Inorganique Moléculaire, URA CNRS 1495, Université de Rennes I, Avenue du Général Leclerc, 35042 Rennes CEDEX, France

$\text{YBa}_2\text{Cu}_3\text{O}_7$ (YBCO) superconducting thin films have been grown *in situ* on single-crystal (1 0 0) MgO substrates by single target d.c. sputtering or laser ablation. The films were highly textured, with full *c*-axis orientation, as shown by standard θ – 2θ X-ray diffractometry. The in-plane structure of the films was characterized by reflection high energy electron diffraction (RHEED), oscillating single-crystal photographs, Rutherford backscattering spectrometry (RBS) and by electron channelling patterns (ECP). According to the results obtained from all these methods the films were found to be single-crystal-like. Channelling RBS experiments were carried out in order to provide additional information on the crystal quality, quantitatively evaluated from the χ_{\min} values: for samples deposited in optimized conditions, we have found these values on sputtered films as well as on laser ablated films deposited on (1 0 0) MgO substrates to be close to that of the virgin substrate. These values strongly depend on the deposition temperature, in good agreement with ECP data. On the other hand, RBS analysis gives access to the composition of the thin films and in addition the in-depth homogeneity in composition was checked by secondary ion mass spectrometry (SIMS).

1. Introduction

Thin films of the high- T_c superconductors have been the subject of many studies for practical developments [1]. In particular, microwave applications are expected soon and for this purpose it is of primary importance to control the growth parameters of the thin films on which would strongly depend the surface resistivity, required to be as low as possible. We have studied thin films deposited on (1 0 0) MgO substrates by two different techniques: single target d.c. sputtering and laser ablation. In this paper we compare the results obtained by Rutherford backscattering spectrometry (RBS) to those obtained by a microscopic analysis, the electron channelling pattern (ECP) method.

2. Deposition procedure

The details of the deposition procedure, that we briefly

summarize below, have been reported elsewhere [2, 3].

Single crystal (1 0 0) MgO substrates used in this work were standard production forms [4] and had not been specially selected. Prior to deposition, they were cleaned using a standard procedure: degreasing in acetone with ultrasonic aid, outgasing *in situ* near 700 °C under secondary vacuum and then under about 0.1 mbar of oxygen. In some cases they were first polished with 0.25 μm diamond paste, and this stage was shown to improve significantly the surface quality with regard to as-supplied samples [5].

2.1. Sputtering deposition

The films were d.c. sputtered onto the single crystal MgO substrates placed on a stainless steel holder which could be heated to about 700 °C. The substrate was placed at a distance of 1.5 cm directly in front of a

* Present Address: Institut de Physique, Université des Sciences et de la Technologie "Houari Boumediene" BP 32, El Alia, Alger, Algeria.

† Present Address: SINTEF Applied Physics, Norwegian Institute of Technology, N-7034 Trondheim, Norway.

‡ Author to whom correspondence should be addressed.

1:2:3 stoichiometric target ($\text{YBa}_2\text{Cu}_3\text{O}_7$). The sputtering gas was a flowing mixture of Ar and O_2 (about 10 %) which was maintained at a pressure of 1.5–2 mbar. Under these conditions the deposition rate was between 0.5 and 1.0 nm min^{-1} . After deposition the samples were slowly cooled in an O_2 atmosphere and no further processing was required.

2.2. Laser ablation

An XeCl excimer laser beam ($\lambda = 308 \text{ nm}$) with a pulse duration of 40 ns (SOPRA SEL 520) was focused onto a very dense ($\geq 90\%$ of the theoretical density) stoichiometric rotating target of YBCO which was at 45° with respect to the beam. The substrate was fixed onto a stainless steel holder which was heated to about 700–750 $^\circ\text{C}$ during deposition. The substrate directly faced the target and was usually kept at 4.5 cm from the target. The deposition was carried out under an O_2 flow at a constant pressure of about 0.3 mbar. The laser operated at a frequency of 3 Hz with an energy by pulse between 80 and 200 mJ. Under these conditions the deposition rate reaches $\sim 10 \text{ nm min}^{-1}$. As for the sputtered films, after deposition the films were cooled to room temperature in an oxygen atmosphere and no post-treatment was performed.

3. Superconducting behaviour

Before discussing the structural characterization of the thin films we will first briefly describe their superconducting behaviour, systematically studied by standard four probe resistive measurements and by a specific inductive method described elsewhere [6].

The superconducting properties of the films deposited by the two techniques are quite similar. In both cases the superconducting transitions are very narrow: typically the full width at half maximum (FWHM) of the transition is lower than 1 K, even for the inductive measurements which are specially sensitive to the homogeneity of the sample. The critical temperature T_{c0} , defined at $R = 0$, is routinely found up to 90 K for the laser ablated films, and a few degrees lower for the d.c. sputtered films. The critical current densities, J_c , estimated by transport measurements are near 10^6 A cm^{-2} at 77 K. We have also evaluated the order of magnitude of J_c by magnetization measurements, using the Bean model, to $\sim 10^7 \text{ A cm}^{-2}$ at 8 K (in all cases the values are indicated without applied magnetic field).

4. Composition

The composition of the deposited films has been routinely determined by energy dispersive spectroscopy (EDS) but this method is not well suitable for very thin films because of the emitting volume depth ($\sim 1 \mu\text{m}$). To obtain more quantitative composition, we have performed RBS analyses at room temperature using a 1 mm diameter spot beam of 1.8 MeV or 2 MeV helium ions generated by a Van de Graaff accelerator. Due to the light masses of the substrate elements (O:16, Mg:24), the backscattering yields

from the substrate can be easily separated from those of the film, as can be seen in Fig. 1. The single masses can be resolved if the film is thin enough, as shown by the RBS spectrum in Fig. 1a of a 67 nm film of YBCO (sample S1). Compare this to the RBS spectrum of a 112 nm YBCO film (sample S2) in Fig. 1b: now the peaks are no longer resolved. The film composition and the thickness were determined from the peak area and the peak width measurements associated with each element. The metal ratios Y:Ba:Cu are determined on the basis of a total of 6 ($1 + 2 + 3$) metal atoms.

From the RBS spectra, the chemical composition of Ba and Cu relative to the Y element was found, for the sputtered YBaCuO films on (100)MgO (example of sample S1), to be close to 1.0:1.9:3.1 stoichiometry with a maximum deviation of 5% in the relative concentrations.

We have found for laser ablated thin films metal ratios near 1.2:1.8:2.9. This composition is very close to the one determined as the optimum one for high critical temperature and current density by H. Jhans *et al.* [7]. In fact, structural and physical characterizations have confirmed that these laser ablated films are of high quality.

Secondary ion mass spectroscopy was carried out to obtain qualitative depth distribution of the laser ablated thin films elements (Y, Ba, Cu). The in-depth distribution of the various species is presented

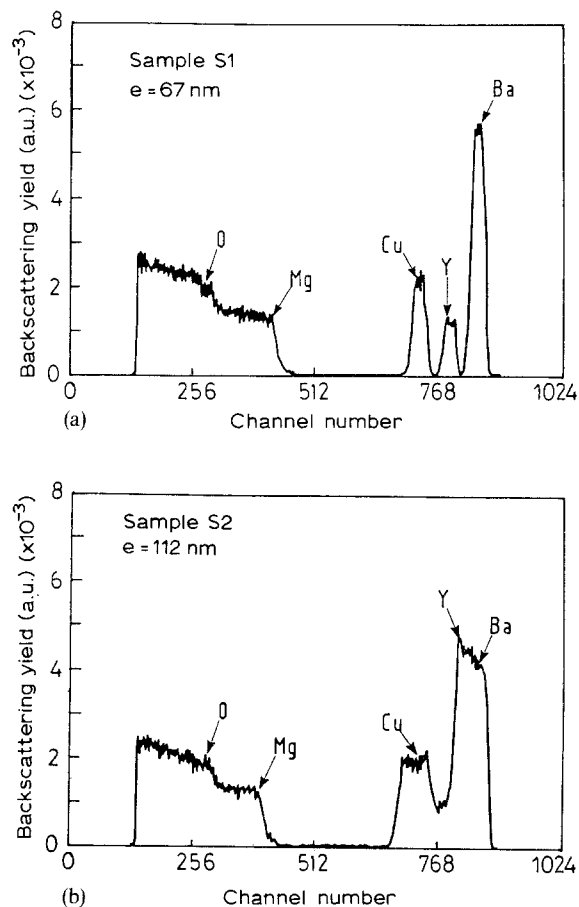


Figure 1 RBS spectra for two different thicknesses of $\text{YBa}_2\text{Cu}_3\text{O}_7$ films deposited on (100) MgO by d.c. sputtering: (a) 67 nm and (b) 112 nm.

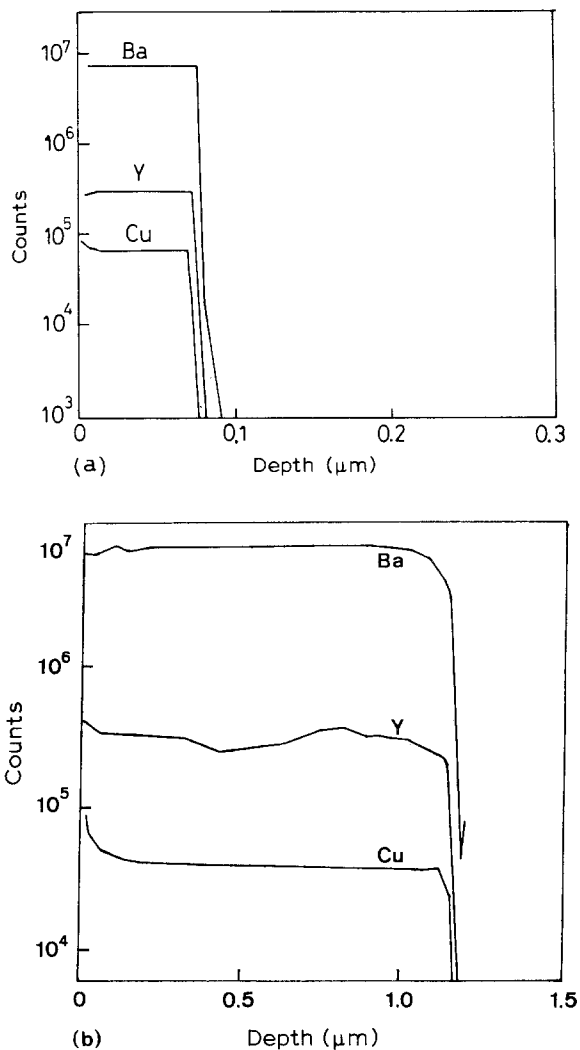


Figure 2 SIMS depth profiles analysis for two $\text{YBa}_2\text{Cu}_3\text{O}_7$ films *in situ* deposited on (100) MgO by laser ablation: (a) for an 86 nm thick film and (b) for a 1100 nm thick film.

in Fig. 2 for a < 100 nm YBCO film (sample L1) and for a largely thicker one (sample L2) deposited on (100)MgO.

The flatness of these SIMS profiles is characteristic of the very good homogeneity across both the 86 nm thin film and the 1100 nm thick film (Fig. 2).

5. Crystalline quality

A large lattice mismatch (about 9 % and 8 % for the a and b directions, respectively) exists between the MgO substrate and the YBaCuO films. Accordingly a strain-free growth is not expected and the crystalline characterization of the film is of primary interest.

We have systematically studied the films by standard θ - 2θ X-ray diffraction (Bragg-Brentano geometry). This method gives information perpendicular to the plane of the sample. The diffractogram corresponding to a typical sample is shown in Fig. 3a. Only the 001 type reflections are observed, meaning that the c -axis is perpendicular to the MgO substrate for all these films, deposited either by d.c. sputtering or laser ablation. We have also recorded θ -scans, also called "rocking curves" for a principal diffraction peak of the film and for the (200) peak related to the

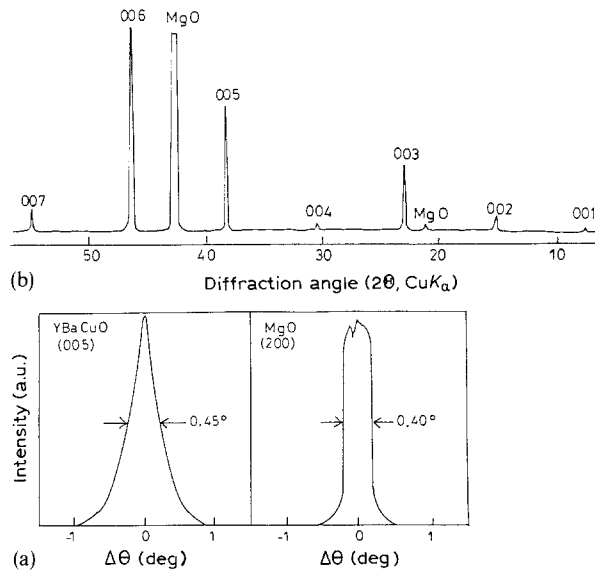


Figure 3 X-ray diffractogram of a typical $\text{YBa}_2\text{Cu}_3\text{O}_7$ film *in situ* deposited on (100) MgO substrate (bottom), and rocking curves about the 005 reflection of the film (top left) and about the 200 reflection of its corresponding substrate (top right).

substrate. The narrowness of the rocking curves, which give information about the mosaicity of the samples, indicates the good crystalline quality of the films (Fig. 3b).

X-ray diffraction data obtained in the oscillating crystal mode [8] or in the fixed sample mode (Fig. 4a) show that the film is quasi single-crystal-like (patterns present no rings, but only defined spots, arranged in rows in the case of oscillating crystal photographs) and that the crystalline axes of the YBaCuO film are aligned with those of the substrate, so that we can conclude that the growth is epitaxial in spite of the mismatch between the film material and the substrate. The RHEED diffraction patterns we obtained on the different films also confirm the epitaxial growth, i.e. the alignment of the film and substrate axes. Our laser deposition chamber is equipped with a RHEED analyser, in contrast to the d.c. sputtering one, so that the RHEED is systematically performed *in situ* after deposition of the laser ablated films [3] and the narrowness of the streaks is characteristic for the "atomically" flat surface of the film (Fig. 4b, sample L3). In the case of sputtered films we must outgas the film at $\sim 700^\circ\text{C}$ under vacuum to clean its surface so that we can observe the RHEED patterns, but the photographs are usually less sharp than the *in situ* observations. The superconducting properties are of course destroyed, so only a few samples have been studied. Nevertheless, we have in both cases obtained patterns characteristic of atomically smooth surfaces.

The RBS and channelling technique has been used in order to evaluate more quantitatively the crystalline growth quality of the YBaCuO films. The minimum yield value χ_{min} , defined as the ratio of the yields in the aligned and random spectra, is in fact a quantitative measurement of the degree of single crystallinity.

In addition we have used ECP (Electron Channelling Pattern) to further characterize the epitaxy [9]. This method uses the rocking of the electron

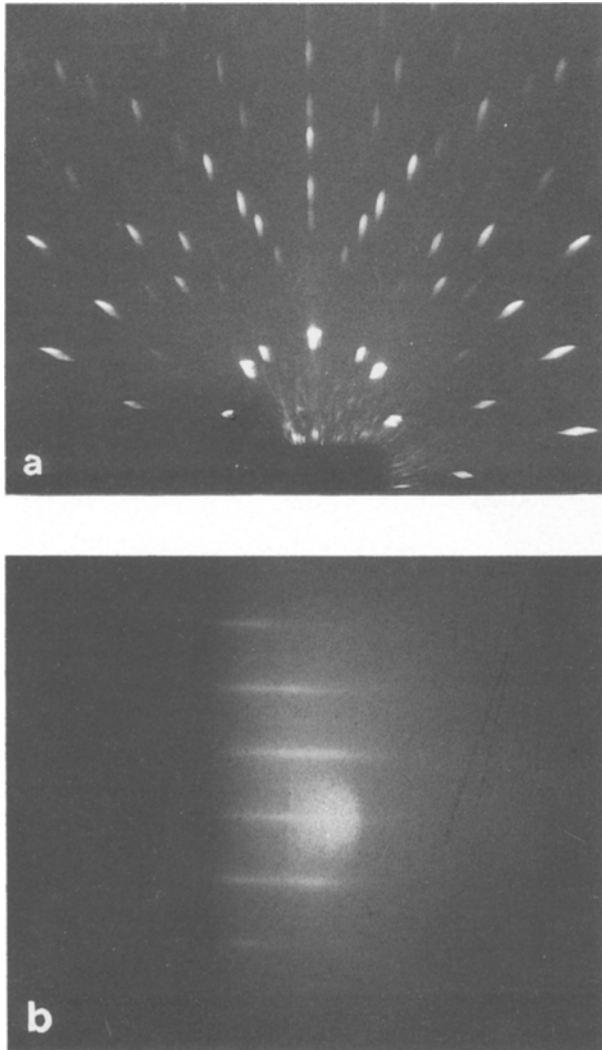


Figure 4 (a) X-ray diffraction photograph of a typical *c*-axis epitaxially grown $\text{YBa}_2\text{Cu}_3\text{O}_7$ film deposited on (100) MgO substrate: notice the absence of any ring. (b) RHEED pattern of an epitaxial $\text{YBa}_2\text{Cu}_3\text{O}_7$ film (sample L3) deposited on (100) MgO corresponding to the $\langle 100 \rangle$ azimuth for both the film and the substrate: notice the narrowness of the streaks.

beam which impinges on a “single-crystal” surface around its normal. Each time the electron beam is in the Bragg position, the yield of backscattered electrons is slightly reduced. Each family of crystallographic planes, normal or slightly tilted with respect to the surface, gives a stripe, the azimuth of which is the trace of the plane. These stripes cross along the crystallographic “pole” corresponding to the axis parallel to the beam. Any misalignment of the crystallites forming the film with respect to each other will result in a rotation of the individual “pseudo Kikuchi” lines, strongly decreasing the sharpness of the pattern. So this qualitative, but quick and easy to use method, is very sensitive to the in-plane perfection of the film crystallization. Moreover this technique is an *ex situ* and fully non-destructive method.

5.1. Sputtered films

The χ_{\min} values of the YBCO films, determined by RBS, were found to depend on the deposition condi-

tions, especially on the deposition temperature. The best value for our sputtered films, measured on a 57 nm thick high quality film, is 16% (sample S3), of the same order of magnitude as the virgin MgO substrate (10.5%). To our knowledge, the best minimum yield values observed up to now for YBaCuO thin films deposited on highest quality (100) MgO substrates are 7% [10] and 3% [1]. So this value of 16% determined behind the Ba surface peak confirms the good crystallinity of the film insofar as it strongly depends on the substrate surface quality [11]. In contrast, a χ_{\min} value of 50% was found for an YBaCuO film of similar thickness obtained under non-optimized deposition conditions (sample S4, deposited at a lower temperature than the optimized one).

We have compared these results to ECP photographs. We have found, as expected, a correlation between the quantitative analysis (RBS in the channelling configuration compared to the random one) and the ECP qualitative analysis based at first on the visual evaluation of the contrast and the definition of the pattern. Fig. 5 (b and c) shows the photographs corresponding to the ECP analysis of two films with χ_{\min} values of 16 and 50%, respectively (S3 and S4), compared to that obtained on a virgin substrate (Fig. 5a). The photographs differ strongly, as in the first case we can see a quite sharp ECP diagram (Fig. 5b) whereas for the 50% χ_{\min} film, which appears only textured by oscillating crystal X-ray diffraction, we cannot distinguish any feature. The rings observed on the photographs could be due to a surface layer, because of long storage of the films without any special precautions (~ 2 years). So this non-destructive microscopic method gives important information about the crystallinity of the thin films and is complementary to methods like RBS.

5.2. Laser ablated films

We have also analysed laser ablated YBaCuO thin films deposited on (100) MgO by RBS and ECP. Fig. 6 shows the random and aligned RBS spectra corresponding to an 81 nm thick film (L3). Again the channelling effect is clearly demonstrated by the χ_{\min} value, determined again at 16% (Fig. 7a) and confirms the good crystallinity of the film. We have measured this value on high quality films that we obtain routinely and not on a specially selected one. So this value of 16%, of the same order of magnitude as the value corresponding to the virgin MgO substrate, measured on several laser ablated films, attests the actual crystalline quality of our films.

We have studied this same film (L3) by ECP. The photograph displayed in Fig. 5d shows a sharp diagram characteristic of high crystalline quality. The rings we can see at the center of the photograph could be due to an adsorbed surface layer; however this sample is more recent and for laser ablated thin films the rings on ECP diagrams are more likely to be caused by the presence of some droplets on its surface, specific to the laser ablated films [12].

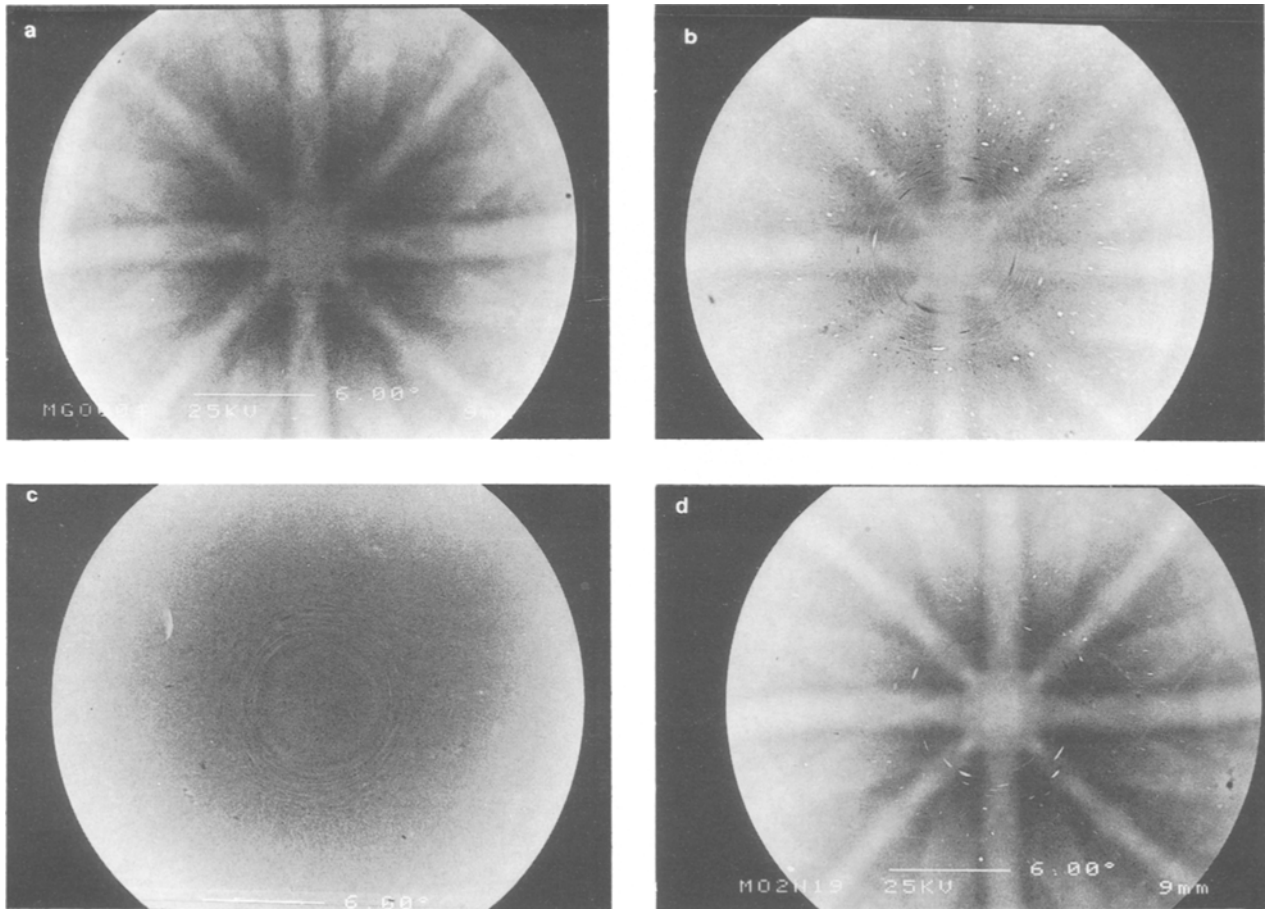


Figure 5 Wide angle electron channelling patterns around the [001] pole of: (a) a virgin single-crystal (100) MgO substrate; (b) an epitaxial $\text{YBa}_2\text{Cu}_3\text{O}_7$ film *in situ* deposited by d.c. sputtering with $\chi_{\min} = 16\%$ (sample S3); (c) a simply textured $\text{YBa}_2\text{Cu}_3\text{O}_7$ film *in-situ* deposited by d.c. sputtering with $\chi_{\min} = 50\%$ (sample S4); (d) an epitaxial $\text{YBa}_2\text{Cu}_3\text{O}_7$ film *in-situ* deposited by laser ablation with $\chi_{\min} = 16\%$ (sample L3).

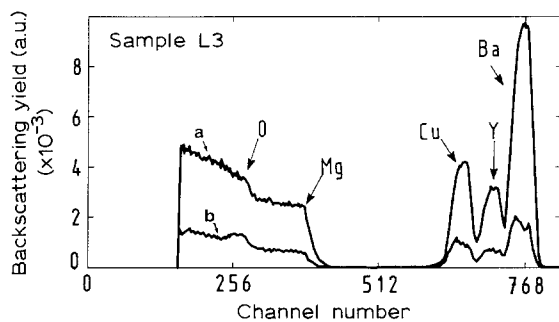


Figure 6 Random (a) and aligned (b) RBS spectra for a 81 nm thick film *in-situ* deposited by laser ablation.

Because of the large lattice mismatch between MgO and YBaCuO , during the initial stage of growth the lattice parameters of the film *a* and *b* tend to expand so as to match the larger lattice constant of MgO, and the *c*-axis will be compressed according to the Poisson effect. This compression will slightly change the angle between the [301] direction in the film and the [101] direction in the substrate. So, angular scans through the inclined crystal direction have been performed on an 81 nm thick film and the results are presented in Fig. 7b. The observed difference in the minima of the scan of about 0.5° can be attributed to the deviation of the [301] film direction from the [101] substrate

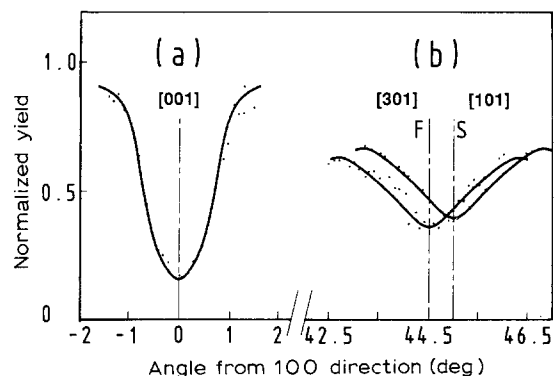
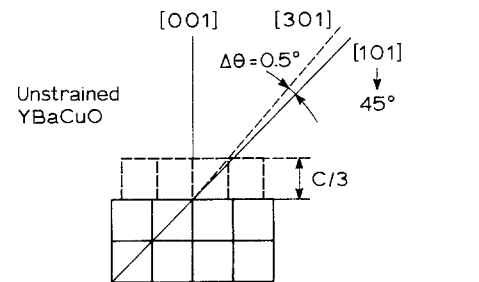


Figure 7 Normalized angular yield profiles of 1.8 MeV He^+ through the [001] (a) and [301] (b) directions for the $\text{YBa}_2\text{Cu}_3\text{O}_7$ film from Fig. 6. In (b) the angle between the [301] direction of the film and the [101] direction of the substrate is clearly shown. The schematic drawing at the top of the figure gives the expected geometry for an unstrained model.

direction calculated for an unstrained film (schematic drawing Fig. 7) and not as a result of a mismatch-induced strain. These results indicate that the YBCO orientation is imposed by that of MgO but that the 81 nm film is relaxed, as expected for the epitaxial growth of a system with a large lattice mismatch. We find the expected value of 0.5° between the $[301]$ film and the $[101]$ MgO directions in good agreement with results previously reported by J. Geerk *et al.* [13] for a YBaCuO film grown on (100) MgO by inverted cylindrical magnetron sputtering, or more recently by H. Jhans *et al.* [7] for a film deposited by e-beam co-evaporation.

6. Conclusion

In summary, in addition to conventional θ - 2θ X-ray diffraction, oscillating single-crystal diffraction and RHEED, we have applied two channelling methods to further characterize crystal growth of our films, deposited either by d.c. sputtering or laser ablation. It has been shown that ion channelling and random RBS spectrometry provide valuable information on the behaviour of the films elements and on many aspects of the synthesis and analysis of epitaxial growth quality of YBaCuO films on (100) MgO substrates. The superconducting properties of the films depend strongly on their epitaxial quality, determined by the minimum yield value, χ_{\min} .

R. P. Sharma *et al.* have extensively studied ion channelling along the $[301]$ and also $[331]$ axes in twinned single crystal $\text{YBa}_2\text{Cu}_3\text{O}_7$ [14]. They observed along the $[301]$ as well as the $[\bar{3}01]$ directions an indication of a double dip, at a separation of $\sim 0.9^\circ$, in excellent agreement with the calculated rotation, 0.96° , of the a and b directions for two adjacent domains in the twin model. In contrast we, as well as other groups [7, 13], did not observe this behaviour in these c -axis oriented films. We would like to emphasize that in the single-crystal, the twin boundaries are parallel to each other and control the misalignment of adjacent subsets of twin variants. In contrast, our films clearly exhibit the presence of small crystallites, about $100 \times 100 \times d \text{ nm}^3$ (d being the film thickness), as previously shown by cross-section SEM observation of cleaved specimens [15] and recently confirmed by scanning tunnelling microscopy (STM) experiments [16] which have displayed "spiral mountains" with screw dislocations similar to those previously reported [17, 18]. Taking into account these small dimensions one can expect that these crystallites are untwinned and that the films are in fact formed by single crystals with the a and b directions statistically interchanged, but forced by the epitaxial growth to remain aligned with the substrate unit-cell axes. The $[301]$ and $[\bar{3}01]$ directions of individual crystals are of course observed simultaneously. Moreover the $[301]$ χ_{\min} value appears very sensitive to the presence of twins. On twinned single crystals it is as large

as $\sim 40\%$ (and is improved to 18% by removing most of the twins) whereas the minimum yield along the $[001]$ direction was only 1.5% [14]. In our experiments these two values are considerably closer, about 37% and 16%, respectively, supporting again the switched untwinned crystals collection hypothesis.

The electron channelling pattern data which give qualitative—but very sensitive to any misalignment—information on crystal quality are in very good agreement with our diffraction and RBS results. These methods complement each other, mainly because of the difference in the depth analysis, of the order of microns for X-ray diffraction, a few hundred nanometres for RBS, some tens of nanometres for ECP and a few nanometres for RHEED. We have shown that it is necessary to measure a low χ_{\min} to observe an electron channelling pattern. For a χ_{\min} of 16% we can see a sharp ECP diagram, whereas for a χ_{\min} of 50% we cannot observe any feature on the ECP photograph.

References

1. D. B. CHRISSEY and A. INAM, *M.R.S. Bull* **17** (1992) 37.
2. M. GUILLOUX-VIRY, M. G. KARKUT, A. PERRIN, O. PEÑA, J. PADIOU and M. SERGENT, *Physica C* **166** (1990) 105.
3. M. G. KARKUT, M. GUILLOUX-VIRY, A. PERRIN, J. PADIOU and M. SERGENT, *Physica C* **179** (1991) 262.
4. M. GUILLOUX-VIRY, C. THIVET, M. G. KARKUT, J. PADIOU, O. PEÑA, A. PERRIN, M. SERGENT, M. GAUNEAU, *Mater. Sci. Eng.* **B18** (1993) 115.
5. Société d'Équipement Industriel du vide (SEI), La Tour-du-Pin, France.
6. O. PEÑA, *Meas. Sci. Technol.* **2** (1991) 470.
7. H. JHANS, L. G. EARWAKER, N. G. CHEW, J. A. EDWARDS and A. G. CULLIS, *Nucl. Instr. Meth. Phys. Res. B* **56/57** (1991) 768.
8. A. PERRIN, M. G. KARKUT, M. GUILLOUX-VIRY and M. SERGENT, *Appl. Phys. Lett.* **58** (1991) 412.
9. A. PERRIN, M. GUILLOUX-VIRY, C. THIVET, J. C. JEGADEN, M. SERGENT and J. LE LANNIC, *Jeol News*, **30E** (1992) 26.
10. Q. LI, O. MEYER, X. X. XI, J. GEERK and G. LINKER, *Appl. Phys. Lett.* **55** (1989) 310.
11. Q. LI, F. WESCHENFELDER, O. MEYER, X. X. XI, G. LINKER and J. GEERK, *J. Less-Common Metals* **151** (1989) 295.
12. G. KOREN, A. GUPTA, R. J. BASEMAN, M. I. LUTWYCHE, R. B. LAIBOWITZ, *Appl. Phys. Lett.* **55** (1989) 2450.
13. J. GEERK, G. LINKER, O. MEYER, Institut für Festkörperphysik, Kernforschungszentrum Karlsruhe, Report (August 1989).
14. R. P. SHARMA, L. E. REHN, P. M. BALDO, U. WELP, Y. FANG, *Phys. Rev. B* **44** (1991) 2334.
15. M. GUILLOUX-VIRY, M. G. KARKUT, A. PERRIN and M. SERGENT, *Mater. Lett.* **10** (1990) 126.
16. A. CATANA, C. ROSSEL, A. PERRIN, M. GUILLOUX-VIRY, C. THIVET, to be published.
17. I. D. RAISTRICK, M. HAWLEY, R. J. HOULTON, J. G. BEERY, *Bull. Amer. Phys. Soc.* **36** (1991) 368.
18. J. G. BEDNORZ, *Bull. Amer. Phys. Soc.* **36** (1991) 487.

Received 22 September 1992
and accepted 11 January 1993